

RESEARCH

Open Access



# *Chlamydia trachomatis* plasmid-encoding Pgp3 protein induces secretion of distinct inflammatory signatures from HeLa cervical epithelial cells

Heng Choon Cheong<sup>1</sup>, Yi Ying Cheok<sup>1</sup>, Yee Teng Chan<sup>1</sup>, Ting Fang Tang<sup>1</sup>, Sofiah Sulaiman<sup>2</sup>, Chung Yeng Looi<sup>3</sup>, Rishein Gupta<sup>4</sup>, Bernard Arulanandam<sup>4,5</sup>, Li-Yen Chang<sup>1</sup> and Won Fen Wong<sup>1\*</sup>

## Abstract

**Background** Genital *Chlamydia trachomatis* infection is the most common bacterial sexual transmitted disease that causes severe complications including pelvic inflammatory disease, ectopic pregnancy, and infertility in females. The Pgp3 protein encoded by *C. trachomatis* plasmid has been speculated to be an important player in chlamydial pathogenesis. However, the precise function of this protein is unknown and thus remains to be thoroughly investigated.

**Methods** In this study, we synthesized Pgp3 protein for in vitro stimulation in the HeLa cervical carcinoma cells.

**Results and conclusion** We showed that Pgp3 induced prominent expression of host inflammatory cytokine genes including interleukin-6 (*IL-6*), *IL-8*, tumor necrosis factor alpha-induced protein 3 (*TNFAIP3*), and chemokine C-X-C motif ligand 1 (*CXCL1*), implying a possible role of Pgp3 in modulating the inflammatory reaction in the host.

**Keywords** *Chlamydia trachomatis*, Pgp3, Cytokine, Chemokine, *IL-6*, *IL-8*, *TNFAIP3*, *CXCL1*

## Introduction

*Chlamydia trachomatis* is an obligate intracellular pathogen that predominantly infects the mucosal epithelial cells lining lower regions of the female reproductive tract. Genital chlamydial infection represents an important

public health concern and is a significant cause of morbidity across the globe with 131 million cases being reported annually [1]. Various adverse obstetrics and gynecological outcomes are associated with chlamydial infection such as preterm delivery, premature rupture of membranes, and spontaneous abortion [2–5]. Although it is widely believed that chlamydial diseases are the results of chronic and overt inflammation in response to chlamydial infection, the precise mechanism whereby these immune responses are produced, and the specific chlamydial antigen that initiates the destructive aspect of such reaction remain poorly understood [6].

Almost all characterized strains of *C. trachomatis* naturally carry a conserved 7.5 kbp plasmid [7]. A total of eight open reading frames (ORFs) have been identified in the chlamydial plasmid, each (*Pgp1–8*) is expressed during infection [8]. The *Pgp3* gene specifies a 28 kDa protein

\*Correspondence:

Won Fen Wong  
wonfen@um.edu.my

<sup>1</sup> Department of Medical Microbiology, Faculty of Medicine, Universiti Malaya, 50603 Kuala Lumpur, Malaysia

<sup>2</sup> Department of Obstetrics and Gynecology, Faculty of Medicine, Universiti Malaya, 50603 Kuala Lumpur, Malaysia

<sup>3</sup> School of Biosciences, Faculty of Health and Medical Sciences, Taylor's University, 47500 Subang Jaya, Selangor, Malaysia

<sup>4</sup> South Texas Center for Emerging Infectious Diseases, University of Texas at San Antonio, San Antonio, TX, USA

<sup>5</sup> Department of Immunology, Tufts University School of Medicine, Boston, MA 02111, USA



© The Author(s) 2023. **Open Access** This article is licensed under a Creative Commons Attribution 4.0 International License, which permits use, sharing, adaptation, distribution and reproduction in any medium or format, as long as you give appropriate credit to the original author(s) and the source, provide a link to the Creative Commons licence, and indicate if changes were made. The images or other third party material in this article are included in the article's Creative Commons licence, unless indicated otherwise in a credit line to the material. If material is not included in the article's Creative Commons licence and your intended use is not permitted by statutory regulation or exceeds the permitted use, you will need to obtain permission directly from the copyright holder. To view a copy of this licence, visit <http://creativecommons.org/licenses/by/4.0/>. The Creative Commons Public Domain Dedication waiver (<http://creativecommons.org/publicdomain/zero/1.0/>) applies to the data made available in this article, unless otherwise stated in a credit line to the data.

that is produced as a stable trimer during infection. As opposed to the other seven plasmid proteins that are localized strictly within the chlamydial inclusions, Pgp3 is secreted into the host cell cytosol or remain in association with the chlamydial outer membrane complex (COMC) during infection [9, 10]. Pgp3 is highly immunogenic, and most patients infected with *C. trachomatis* develop antibodies to the protein, suggesting its possible involvement in the development of host immunopathology [11–14].

In this present study, we examined the cellular responses following Pgp3 stimulation. Our results showed that Pgp3 induced prominent expression of several genes encoding pro-inflammatory cytokines including interleukin 6 (*IL-6*), interleukin 8 (*IL-8*), and C-X-C motif chemokine ligand 1 (*CXCL1*). Tumor necrosis factor, alpha-induced protein 3 (*TNFAIP3*), a gene with a known role in immunosuppression was also upregulated, suggesting a role of Pgp3 in the modulation of host immune responses.

## Materials and methods

### *C. trachomatis* infection

Hela-229 cells (ATCC CCL-2.1) were infected with *C. trachomatis* Serovar D (ATCC VR-885) using a method previously described with minor modifications [15]. Briefly, confluent monolayer cells were washed with Hank's Balanced Salt Solution (HBSS) and then treated with Diethylaminoethyl (DEAE)-dextran (30 µg/mL) in HBSS for 35 min prior to infection. DEAE-dextran treated cells were infected with *C. trachomatis* resuspended in sucrose phosphate glutamate buffer (SPG), followed by incubation in a shaking incubator with constant shaking for 2 hr. After that, Dulbecco's Modified Eagle Medium (DMEM) supplemented with 10% fetal bovine serum (FBS), 10 µg/mL gentamicin, and 1 µg/mL

cycloheximide was added to the flask and the cells were incubated at 37 °C, 5% CO<sub>2</sub> for 72 hr.

### Pgp3 cloning

*C. trachomatis* DNA was extracted based on procedures outlined previously with modifications [16]. Cells at 72 h post-infection were detached mechanically from the tissue culture flask using 5 mm borosilicate glass beads. The detached cells were further disrupted in a 50 mL centrifuge tube and the resultant lysed cells were centrifuged at 500×g, 4 °C for 10 min to remove cell debris. Then, the supernatant was centrifuged in a high-speed centrifuge at 14,000×g, 4 °C for 90 min. The supernatant was discarded and the pelleted elementary body (EB) was resuspended in 180 µL buffer ATL for DNA extraction using the DNeasy Blood & Tissue kit (Qiagen, Hilden, Germany). In brief, the resuspended EBs were first mixed with 20 µL Proteinase K and then incubated in a dry block heater at 56 °C for 3 hr. After adding 200 µL Buffer AL and 200 µL 100% ethanol, the mixture was centrifuged through a DNeasy Mini spin column. The spin column was washed, and DNA was eluted with 100 µL Buffer AE and then kept at –20 °C prior until further processing.

Chlamydial *Pgp3* gene was obtained from the extracted *C. trachomatis* DNA using gene-specific primer pairs as described previously with modifications to the restriction sites as outlined in Table 1 [9]. Amplification was performed using Q5 high-fidelity DNA polymerase (New England Biolabs, MA, USA) using the following cycling profile: 95 °C for 5 min, 35 cycles of 95 °C for 30 sec, and 60 °C for 45 sec. The amplicons were ligated into the vector pTriEx-3 Hygro (Novagen, NJ, USA) with 8× histidine residues fused to the C-terminus and subsequently transformed into the *Escherichia coli* cloning host Nova-Blue (Novagen). After sequence verification of positive recombinant clones, the recombinant plasmids were then

**Table 1** Cloning primers of Pgp3 gene and primers used for qRT-PCR analysis of immune-related genes

Target gene	Forward primer (5'-3')	Reverse primer (5'-3')	Amplicon size (bp)
<i>Pgp3</i>	CATG*CCATGG*GAAATCTCTGTTTATTTG	CGTA/CTCGAG/AGCGTTTGTGAGGT	792
<i>CXCL1</i>	GCGGAAAGCTTGCCCTCAA	TCAGCATCTTTTCGATGATTTCTT	62
<i>GM-CSF</i>	CACTGCTGCTGAGATGAATGAAA	GTCTGTAGGCAGGTCGGCTC	78
<i>IL-1α</i>	TGTATGTGACTGCCCAAGATG	TTAGTGCCGTGAGTTTCCC	121
<i>IL-5</i>	GAGACCTTGGCACTGCTTTC	CAGTACCCCTTGACAGTT	157
<i>IL-6</i>	CCACTCACCTCTTCAGAACG	CATCTTTGGAAGGTTTCAGGTTG	150
<i>IL-8</i>	CCTGATTTCTGCAGCTCTGT	TCTGCACCCAGTTTTCCTTG	221
<i>TNF-α</i>	ACTTTGGAGTGATCGGCC	GCTTGAGGGTTTGCTACAAC	139
<i>TLR2</i>	CAGGTGACTGCTCGGAGTTC	CACAACTACCAGTTGAAAGCAGTGA	171

Restriction sites: \* \*, *NcoI* site; //, *XhoI* site

transformed into the *E. coli* expression host RosettaBlue (DE3) pLacI (Novagen).

### Protein synthesis and purification

Transformed *E. coli* expression host was cultured in selective lysogeny broth containing 50 µg/mL ampicillin, 12.5 µg/mL tetracycline, and 34 µg/mL chloramphenicol supplemented with 1% glucose. Cells were grown at 37 °C with aeration at 250 rpm to an OD<sub>600</sub> of ≥0.7, upon which expression was induced with 1 mM isopropyl β-D-1-thiogalactopyranoside (IPTG). After 4 hr, the bacterial pellets were obtained by centrifugation at 10,000×g for 10 min at 4 °C. The pelleted cells were resuspended in 10 mL lysis buffer (10 mM Na<sub>2</sub>HPO<sub>4</sub>, 10 mM NaH<sub>2</sub>PO<sub>4</sub>, 500 mM NaCl, 2 mg/mL lysozyme, pH 7.4), incubated on ice for 30 min, and then sonicated in a Branson Sonifier 250. The resultant crude lysate was centrifuged at 10,000×g for 10 min at 4 °C and the clarified supernatant containing the soluble proteins was then collected for purification.

Pgp3 protein was purified by immobilized metal affinity chromatography (IMAC) using HisTrap HP column (GE Healthcare, UK) on an AKTA Purifier System (GE Healthcare, UK). Purification of Pgp3 was performed natively by applying the clarified supernatant containing the soluble Pgp3 onto the column pre-equilibrated with binding buffer (10 mM Na<sub>2</sub>HPO<sub>4</sub>, 10 mM NaH<sub>2</sub>PO<sub>4</sub>, 500 mM NaCl, and 20 mM imidazole). Unspecific proteins were removed by washing the column with 5 column volumes of binding buffer and the protein of interest was eluted in elution buffer (10 mM Na<sub>2</sub>HPO<sub>4</sub>, 10 mM NaH<sub>2</sub>PO<sub>4</sub>, 500 mM NaCl, and 500 mM imidazole). The eluted proteins were collected for immunoblot analyses. Eluted Pgp3 fractions desalted using HiTrap desalting column (GE Healthcare, UK) fitted onto an AKTA purifier system (GE Healthcare, UK). Desalted Pgp3 was depyrogenated with Pierce high-capacity endotoxin removal spin column (Thermo Fisher Scientific, MA, USA) in accordance with the manufacturer's protocols. Depyrogenated Pgp3 was further concentrated using Vivaspin 6 centrifugal concentrator (Sartorius AG, Germany). Protein concentration was determined using Pierce BCA protein assay kit (Thermo Fisher Scientific, MA, USA). The concentration of endotoxins present in the depyrogenated Pgp3 was assayed using HEK-Blue lipopolysaccharide (LPS) detection kit 2 (Invivogen, CA, USA). In brief, HEK-Blue cells were added to each well to a concentration of 4 × 10<sup>5</sup> cells/mL and subsequently incubated overnight at 37 °C in a humidified incubator at 5% CO<sub>2</sub> atmosphere. Following overnight incubation, 20 µL of cell supernatants from each standard and unknown were mixed 180 µL of QUANTI-Blue reagent (Invivogen, CA, USA) and incubated for 6 hr at 37 °C. Absorbance at

620 nm was read with a Synergy HTX microplate reader (BioTek Instruments, VT, USA).

### Gel electrophoresis and immunoblotting

Purified Pgp3 was separated with sodium dodecyl sulfate–polyacrylamide gel electrophoresis (SDS-PAGE) and then stained with Coomassie brilliant blue G-250 (Bio-Rad, CA, USA). Native-PAGE was performed with the same procedures as SDS-PAGE, except without heat denaturing and treatments with reducing agents including SDS and β-mercaptoethanol in the experiments. For immunoblot analysis, the separated proteins were blotted onto polyvinylidene difluoride (PVDF) membrane and then blocked with 5% bovine serum albumin (Merck Millipore, MA, USA). Detection of the His-tagged recombinant Pgp3 was carried out by incubating the membrane with HisDectector nickel alkaline phosphatase (AP)-conjugate (KPL, MD, USA) diluted 1:5000 for 1 hr at room temperature. Subsequently, the color was developed by adding NBT-BCIP substrate (Promega, WI, USA).

### Peptide mass fingerprinting

Purified Pgp3 was resolved using SDS-PAGE and then stained overnight with colloidal Coomassie blue G-250 (Bio-Rad, CA, USA). Protein band corresponding to the molecular weight of Pgp3 monomer (~28 kDa) was excised from stained gel. The band was destained, dried, and then digested with trypsin for 2 hr at 37 °C. Digested gel plugs were solvent extracted twice using 0.1% trifluoroacetic acid (Sigma-Aldrich, MO, USA) in 50% acetonitrile for 30 min at room temperature and transferred to new wells. Following overnight drying at 37 °C, the dried peptides were reconstituted with 10 µL of 0.1% formic acid (Sigma-Aldrich, MO, USA). The tryptic peptides were desalted by using ZipTip with 0.1% formic acid and eluted with 0.1% formic acid in 50% acetonitrile. Eluted peptides were mixed with equal volume of matrix solution (6 mg/mL α-cyano-4-hydroxycinnamic acid in 70% acetonitrile, 0.1% formic acid) and spotted onto the sample slide before analyzed on a 5800 Plus Matrix-assisted laser desorption/ionization-tandem time of flight (MALDI TOF/TOF) analyzer (Applied Biosystems/SCIEX, CA, USA). Protein identity was confirmed by searching the Swiss-Prot database using the MASCOT search engine with the following parameters: enzyme – trypsin, missed cleavage – 1, variable modification – 2; (I) carbamidomethylation of cysteine residues, and (II) allowed variable modifications of methionine oxidation, MS precursor ion mass tolerance – 100 ppm, tandem mass spectrometry (MS/MS) fragment ion mass tolerance – 0.2 Da, and mass values restricted to monoisotopic, as previously described [17].

### Cell stimulation

A day prior to stimulation, HeLa-229 cells were seeded at a density of  $1 \times 10^5$  cells/mL in DMEM supplemented with 10% FBS in a 6-well plate and grown overnight at 37°C, 5% CO<sub>2</sub>. The serum containing DMEM was removed, washed once with DPBS, before replacing the medium with serum-free DMEM. After that, cells were treated with Pgp3 at final concentrations of 5 µg/mL and 10 µg/mL. Cells stimulated with DPBS and 0.1 µg/mL LPS were prepared alongside to serve as a negative and positive control, respectively. The cells were incubated for 24 h at 37°C, 5% CO<sub>2</sub> before harvested for extraction of RNA.

### RNA extraction

RNA was extracted from HeLa-229 cells using Trizol reagent (Invitrogen, CA, USA). A total of 1 mL Trizol reagent and 200 µL chloroform was added into cell pellet, vortexed and left for 3 min at room temperature before centrifugation at 12,000×g for 15 min at 4°C. Then, the upper layer of the sample mixture was collected and transferred to a tube containing 400 µL of isopropanol. Sample was then mixed and left for 10 min at room temperature before centrifugation. RNA pellet was washed using 75% ethanol, dissolved in 30 µL of RNase-free water and stored at -80°C until further usage.

### Quantitative real-time polymerase chain reaction (qRT-PCR)

Extracted RNAs were converted to cDNA by using iScript cDNA synthesis kit (Bio-Rad, CA, USA) according to the manufacturer's guidelines. qRT-PCR was performed using Kapa SYBR Fast qPCR master mix (2×) kit (KapaBiosystems, MA, USA). The qRT-PCR master mix comprised 5 µL of Kapa SYBR Fast qPCR master mix (2×), 0.2 µL of each 10 µM forward and reverse primers, 0.2 µL of 50× ROX low, 1 µL of template DNA, and 3.4 µL of water. qRT-PCR was performed using the following cycling parameters: 95°C for 3 min, 40 cycles of 95°C for 3 seconds, 60°C for 20 seconds, and a dissociation curve analysis step consisting of 1 cycle of 95°C for 3 min, 95°C for 3 seconds, and 60°C for 20 seconds. The relative fold change of each gene was calculated using the  $2^{-\Delta\Delta C_T}$  method [18]. All reactions were performed in triplicates and the results were expressed as mean ± standard deviation (SD). The primer sets used in qRT-PCR are listed in Table 1.

### NanoString nCounter analysis

Hybridization of mRNA with both reporter codes and capture probes was carried out as specified by the manufacturer (NanoString Technologies Inc., WA, USA). Following 16 hr incubation at 65°C on a Veriti thermal

cycler (ThermoFisher Scientific, MA, USA), the reaction mix containing 20 ng/µL of RNA, reporter codes, as well as capture probes were transferred to nCounter Prep Station (NanoString Technologies) for processing. The experiment was performed in triplicates from three independent experiments. Gene expressions were analyzed on an nCounter MAX Analysis System using the nCounter PanCancer Pathways Panel for human (NanoString Technologies).

### Expression data and statistical analysis

Data normalization and analysis of gene expression were performed with nSolver analysis software (version 4.0, NanoString Technologies) using the advanced analysis module to calculate the differential expression fold change between samples. Genes with fewer than 30 reads were removed from all samples following normalization of raw data to internal spike-in negative and positive controls as well as reference genes. Heatmap was generated using Morpheus (<https://software.broadinstitute.org/morpheus>). Z-scores were computed from log<sub>2</sub>-adjusted expression data, following which unsupervised hierarchical clustering of genes was performed by using one minus Pearson's correlation matrix with average linkage method in Morpheus. The scale of the expression data is based on the maximum and minimum values of each row. Statistical significance for the NanoString data was conducted using the R-statistics by either log-linear regression or simplified negative binomial model, with *P*-values adjusted according to Benjamini-Hochberg method. Volcano plot was generated using GraphPad Prism 9.0 (GraphPad Software, San Diego, CA, USA) Data were analyzed with unpaired two-tailed Student's *t*-test using GraphPad Prism 9.0 (GraphPad Software) when comparing between two groups. Statistical significance was established when *P* < 0.05\*, *P* < 0.01\*\*, *P* < 0.001\*\*\*, and *P* < 0.0001\*\*\*\*.

## Results

### Expression and purification of chlamydial Pgp3 protein

The *C. trachomatis* Pgp3 protein was synthesized in an *E. coli* expression system and purified from the solution fraction of the cell lysates using immobilized metal affinity chromatography. Expression of recombinant Pgp3 was confirmed by the presence of a protein of approximately 29 kDa bands in SDS-PAGE and immunoblot analyses (Fig. 1, left panel). Majority of the contaminating *E. coli* proteins were removed after purification. When purified product was analyzed on native-PAGE gel, trimer and oligomer bands of Pgp3 can be detected, suggesting native structure of the functional Pgp3 (Fig. 1, right panel).

The identity of the *C. trachomatis* Pgp3 protein was verified by peptide mass fingerprinting using mass

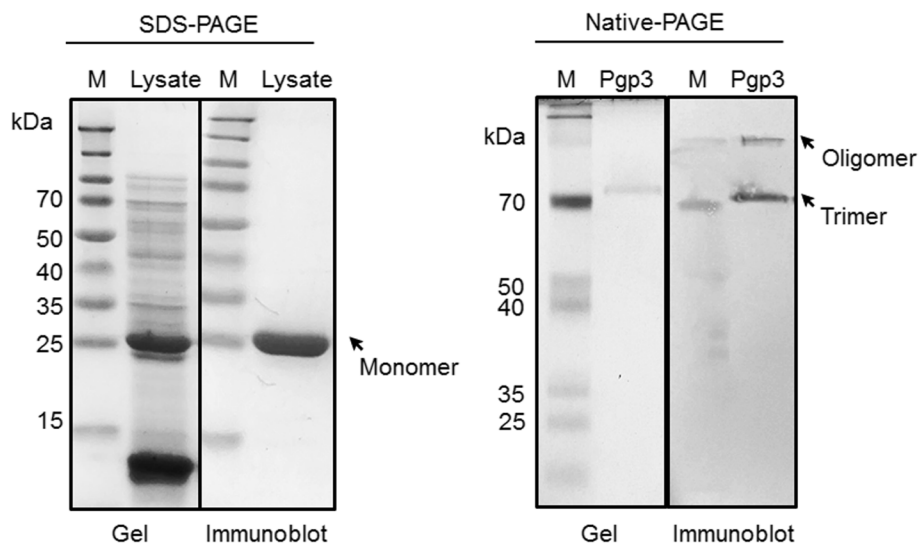


**Fig. 1** Pgp3 protein synthesis and purification. Left panel: SDS-PAGE gel and immunoblot images of the crude cell lysates derived from Pgp3 transfected cells. Right panel: Native-PAGE gel and immunoblot images of the purified soluble Pgp3 protein fraction. His-conjugated protein was detected using HisDectector nickel alkaline phosphatase (AP)-conjugate. M: Protein marker. Arrows show the position of protein band of the expected molecular weight of Pgp3 monomer (~29 kDa), trimer (~80 kDa) and oligomer (>100 kDa)

spectrometry (Table 2), and was subsequently concentrated and depyrogenated. The endotoxin level of purified Pgp3 was <1.0 EU/ $\mu$ g.

#### Transcriptome alterations in chlamydial Pgp3-stimulated HeLa cells

To investigate a broad transcriptomic modification following chlamydial Pgp3 stimulation, cellular total mRNA transcripts in HeLa human cervical epithelial cells were profiled using NanoString nCounter analysis with the nCounter PanCancer Pathways Panel (human code-set) that contains 770 genes with relevant roles in cancer and inflammation. Principal component analysis (PCA) showed a clear separation of clusters according to different treatment groups, indicating distinct mRNA expression profiles of the unstimulated control versus Pgp3-stimulated HeLa cells (Fig. 2A). Overall, a total of 14 significant genes were differentially expressed in the cells exposed to Pgp3 in comparison to untreated controls (Fig. 2B, C). Among the top upregulated genes were those encoding for proinflammatory cytokines, namely *IL8* and *IL6*, which were significantly increased by 1.97- ( $P=0.00183$ ) and 1.18-fold ( $P=0.00194$ ) respectively, following treatment with Pgp3 proteins (Fig. 2B, C).

Additionally, Pgp3 protein also induced significant upregulation of tumor necrosis factor  $\alpha$ -induced protein 3 (*TNFAIP3*) to 1.46-fold ( $P=0.00335$ ). *TNFAIP3* encodes for the ubiquitin-modifying enzyme A20, which plays a role in immune suppression through inhibiting the tumor necrosis factor (TNF)-induced signaling pathways upstream of transcription factor NF- $\kappa$ B and TNF-mediated apoptosis [19, 20]. Although *TNFAIP3* functions to limit inflammation, our finding of chlamydial plasmid-encoded Pgp3 protein augmented *TNFAIP3* agrees with a previous report which infected HeLa cells using plasmid-bearing *C. trachomatis* [21]. This suggests a likelihood of Pgp3 in limiting host immune response during chlamydial infection.

Signal transduction and activator of transcription 1 (*STAT1*), on the other hand, was also increased moderately at 0.88-fold ( $P=0.00797$ ) in response to Pgp3 stimulation (Fig. 2B, C), upregulation of which has previously been found to be crucial for the host anti-chlamydial response [22]. Other genes that showed marginal elevation after Pgp3-treatment include interleukin-1 receptor-associated kinase 2 (*IRAK2*), promyelocytic leukemia (*PML*), ephrin A1 (*EFNA1*), Alkb homolog 3, alpha-ketoglutarate dependent dioxygenase (*ALKBH3*), as well

**Table 2** Pgp3 identification by MALDI-TOF peptide mass fingerprinting

	Approx. band size (kDa)	Mowse score	Sequence coverage (%)	No. of matched peptides	Calculated mass	Expect value
Pgp3	29.1	89	10	2	28,076	0.0064

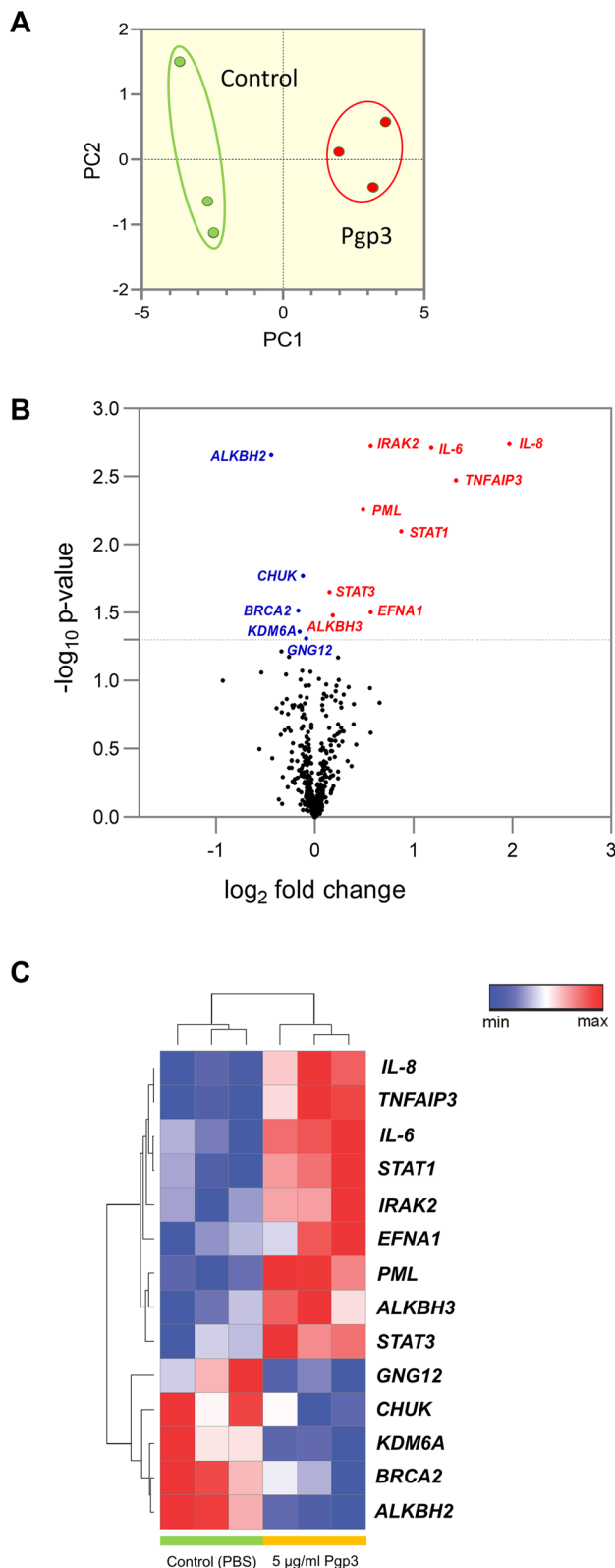


**Fig. 2** NanoString analysis of mRNA expression in Pgp3-treated epithelial cells. **A** Principal component analysis of the NanoString nCounter mRNA expression in epithelial cells following treatment with 5 µg/mL Pgp3 and PBS. **B** Volcano plot displaying differential gene expression caused by Pgp3 between two groups; red: upregulation; blue: downregulation; black: non-significant. **C** A heatmap illustrating unsupervised clustering of statistically significant differentially regulated genes between control (PBS) and 5 µg/mL Pgp3-stimulated epithelial cells; red: upregulation; blue: downregulation

as *STAT3*, at 0.56- ( $P=0.00189$ ), 0.56- ( $P=0.0055$ ), 0.49- ( $P=0.0313$ ), 0.18- ( $P=0.0331$ ), and 0.15-fold ( $P=0.0223$ ) respectively.

Several other significant genes were downregulated modestly in the presence of Pgp3 protein, including Alkb homolog 2, alpha-ketoglutarate dependent dioxygenase (*ALKBH2*), breast cancer 2 (*BRCA2*), lysine-specific demethylase 6A (*KDM6A*), conserved helix-loop-helix ubiquitous kinase (*CHUK*), G protein subunit gamma 12 (*GNG12*), which reduced by 0.442- ( $P=0.0022$ ), 0.17- ( $P=0.0305$ ), 0.15- ( $P=0.0436$ ), 0.15- ( $P=0.0169$ ), and 0.09-fold ( $P=0.049$ ) respectively (Fig. 2B, C).

#### Upregulated expression of IL-6 and IL-8 genes following Pgp3 stimulation

To verify the Nanostring data, mRNA transcripts were investigated using qRT-PCR (Fig. 3). Two of the top upregulated genes i.e. IL-6 and IL-8 were examined along with few other important cytokines. Expressions of both IL-6 and IL-8 were increased significantly in a concentration-dependent manner in response to Pgp3 stimulation. IL-8 was upregulated 0.69-fold ( $P<0.01^{**}$ ) when stimulated with 5 µg/mL of Pgp3, while 10 µg/mL of Pgp3 stimulation caused a 1.25-fold ( $P<0.001^{***}$ ) increase in IL-8 relative to control. Pgp3 stimulations induced 0.48-fold ( $P<0.05^*$ ) and 0.53-fold ( $P<0.01^{**}$ ) increases in IL-6 when compared to unstimulated control.

TLR2 activates signaling pathway which triggers *IL-8* gene transactivation [23]. To examine the involvement of TLR2, we have also examined its expression. The transcript levels of *TLR2* were elevated by 1.1-fold ( $P<0.001^{***}$ ) and 1.01-fold ( $P<0.0001^{****}$ ) upon exposure to 5 µg/mL and 10 µg/mL Pgp3, respectively. This likely suggests that *IL-8* is activated following TLR2 signal activation by Pgp3 (Fig. 3).

No such substantial increase pattern in a dose-dependent manner was detected in other cytokines examined. Expression of *IL-1 $\alpha$* , *IL-12 $\beta$*  and *IFN- $\gamma$*  showed no significant changes following Pgp3 stimulation. *TNF- $\alpha$*  level, on the other hand, was 1.02-fold ( $P<0.05^*$ ) higher when epithelial cells were treated with 5 µg/mL of Pgp3. However,

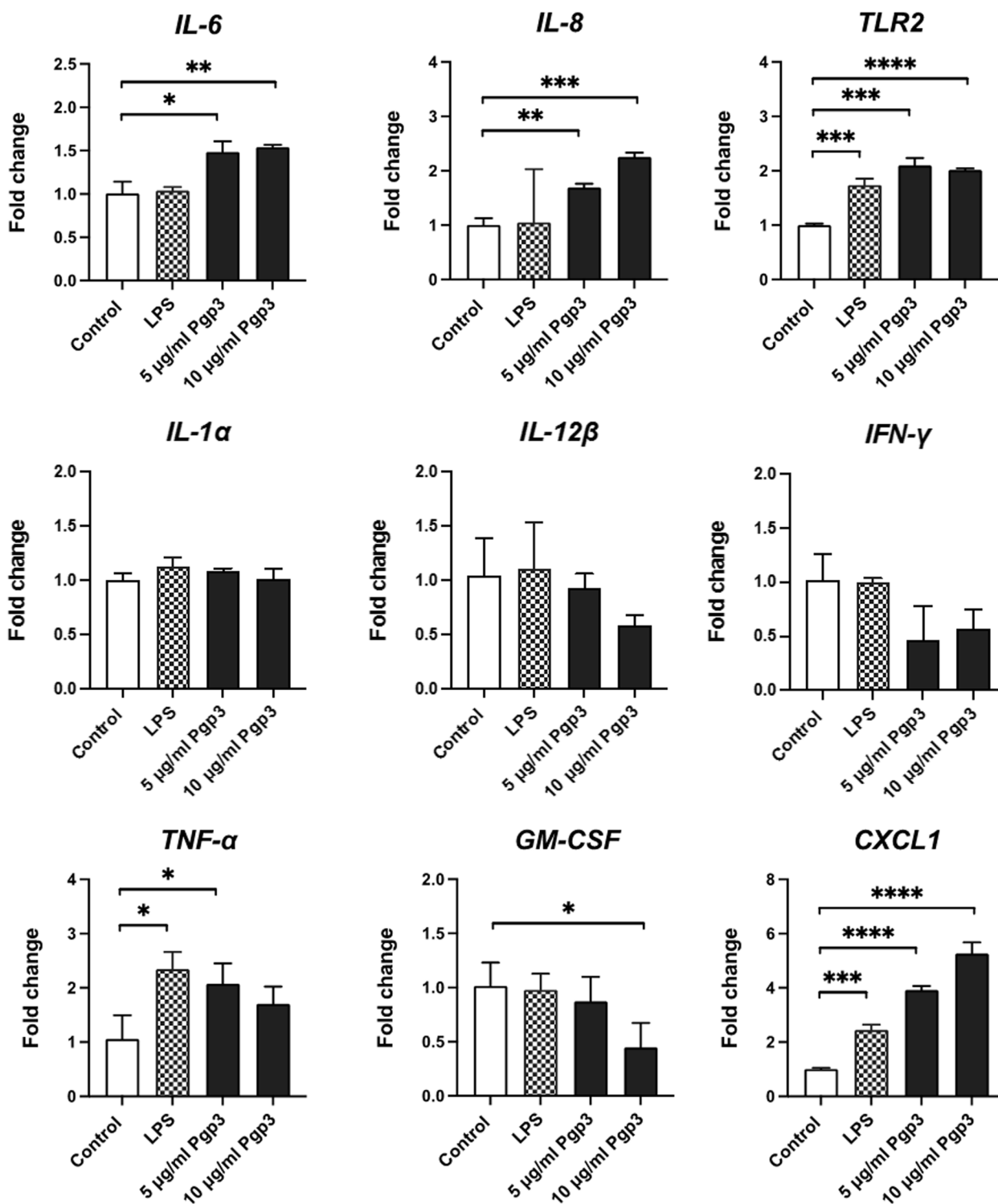


**Fig. 3** qRT-PCR analysis of immune-related genes. The results were expressed as mean ± SD of an experiment in triplicate. The results are representative of two independent experiments where qRT-PCR was performed in triplicate for each sample. Asterisks denote statistical significance by Student's t-test when comparison was made against control.  $P < 0.05^*$ ,  $P < 0.01^{**}$ ,  $P < 0.001^{***}$ , and  $P < 0.0001^{****}$

stimulation of epithelial cells with 10 µg/mL of Pgp3, induced an insignificant increase in *TNF-α* transcripts.

Previous study reported that infection by *C. trachomatis* in epithelial cells triggers release a range of cytokines that include IL-1α, granulocyte-macrophage colony-stimulating factor, (GM-CSF), IL-6, as well as IL-8 [24]. Interestingly, chlamydial Pgp3 protein alone could elicit immune response that results in release of IL-6 and IL-8; but not sufficient to activate IL-1α, GM-CSF and other cytokines examined (Fig. 3). Instead, treatment with high concentration (10 µg/mL) of Pgp3 caused a significant downregulation of *GM-CSF*, with a 0.57-fold ( $P < 0.05^*$ ) decrease in expression versus control. This signifies a specific route of Pgp3 recognition and signaling pathway activation by epithelial cells.

Other than cytokines, *C. trachomatis* infection is known to induce CXCL1 [24]. Similar to previous study, we showed that the expression of *CXCL1* was also increased significantly in a concentration-dependent manner in response to Pgp3 stimulation (Fig. 3). *CXCL1* mRNA transcripts were elevated by 2.92-fold ( $P < 0.0001^{****}$ ) and 4.26-fold ( $P < 0.0001^{****}$ ) compared to control following stimulations with 5 µg/mL and 10 µg/mL of Pgp3, respectively.

## Discussions

In spite of the differences in tissue tropism, several members of the genus *Chlamydia* namely *C. trachomatis*, *C. muridarum*, *C. psittaci*, *C. suis*, *C. caviae*, *C. felis*, *C. pecorum*, along with animal isolates of *C. pneumoniae*, naturally bear a conserved ~7.5 kb plasmid [25–28]. The plasmid is strikingly conserved within *C. trachomatis*, with only ~1–3% nucleotide variation between different strains [29, 30]. Although several isolates of *C. trachomatis* devoid of the plasmid have been identified and characterized, they are considered a rare occurrence, suggesting the presence of strong selective pressure favoring the persistence of plasmid in the environment [31–33]. Interestingly, Pgp3 represents the only one of the seven plasmid proteins that is secreted into the host cell during infection [9]. It is therefore possible that Pgp3 may elicit immune responses from host cells and contribute to the induction of host immunopathology.

Although transcriptomic analyses in the present study did not reveal dramatic differences between the Pgp3-exposed cells and control, our data herein showed that stimulation of epithelial cells with Pgp3 increased the levels of expression of *CXCL1* and *IL-8* in a concentration-dependent manner. In addition, the levels of *IL-6* were increased prominently. Epithelial cells are known to produce various proinflammatory cytokines and chemokines that include *CXCL1*, *IL-6*, *IL-8*, as well as GM-CSF following infection with *C. trachomatis*

[21, 24, 34]. *IL-6*, *IL-8*, *CXCL1* are known to promote neutrophil recruitment during inflammation. However, previous reports suggested that neutrophils were insufficient for clearing chlamydial infection. Importantly, both *IL-8* and *CXCL1*, are capable of delaying apoptosis of neutrophils. Therefore, the retention of neutrophils at the site of infection could lead to the development chronic inflammation which represents a hallmark of chlamydial infection [35–37]. This may be further magnified by other immune cells such as monocytes, which have been shown to elevate the production of *IL-6* and *IL-8* in a co-culture model of chlamydial infection of HeLa and THP-1 cells [38]. Interestingly, infection with plasmid-bearing *C. muridarum* attenuated neutrophil apoptosis in mice, which translated to significantly higher levels of cytokines and increased infiltration of mediator of tissue pathology in comparison with the strain lacking the plasmid [39]. Additionally, loss of the *Pgp3* gene in *C. trachomatis* L2 and *C. muridarum* was correlated with both attenuated infectivity and inflammatory infiltration in murine model of genital tract infection [40, 41]. Such attenuated phenotype was also observed in chlamydial infection using a macaque model of ocular infection [42]. These findings collectively suggest that the chlamydial plasmid serves as a contributor to the host inflammatory response to infection.

Toll-like receptors (TLRs) are components of the innate immune system that recognize microbial derived or endogenous ligands. The recognition of these molecules by TLRs trigger the activation of a cascade of downstream events resulting in inflammatory responses [43, 44]. TLR2 is involved in the host immune defense mechanism towards chlamydial infection and may have a potential role in the induction of chronic inflammatory sequelae as oviduct pathology was attenuated in mice knockout for *TLR2* [45–47]. In vivo studies with *C. trachomatis* and *C. muridarum* have revealed a dependency of the chlamydial plasmid for TLR2 activation. Plasmid loss was accompanied by both lowered in vitro as well as in vivo infectivity and reduced pathology in animals [21, 39, 42, 48–53]. Pgp3 was previously shown to elicit the production of a number of proinflammatory cytokines, such as *TNF-α*, *IL-1β*, and *IL-8* from both mouse Raw 264.7 macrophages and human cell line THP-1. The latter was believed to be dependent on TLR2, activation of which triggers the release of cytokines through the MAPK and (ERK)/MAPK pathways [9, 54]. The data from the current study support these prior findings, whereby parallel increases of both *IL-6* and *IL-8* transcripts were observed with elevation of *TLR2* was observed in response to Pgp3 stimulation. This suggests that Pgp3 is capable of inducing the production of proinflammatory mediators from



epithelial cells possibly by activating TLR2, which could contribute to inflammatory injury.

In addition to *IL-6*, *IL-8*, and *CXCL1*, we observed that Pgp3 caused significant upregulation of *TNFAIP3* in epithelial cells. *TNFAIP3* codes for the ubiquitin-modifying enzyme A20 that possesses an anti-inflammatory function by suppressing the activation of NF- $\kappa$ B [19, 20]. This agrees with Porcella et al. whose team found that plasmid-bearing *C. trachomatis* infection upregulated *TNFAIP3* more significantly compared to its plasmidless counterpart. Our result provides additional evidence to incriminate Pgp3 in the immune evasion during chlamydial infection. It has been demonstrated previously that Pgp3 is able to bind to and forms complex with the human LL-37 peptide, effectively neutralizes the peptide in the process [55]. Produced by both epithelial cells and immune cells such as macrophages and neutrophils, the LL-37 is the sole member of the human cathelicidin protein family and is known to have antimicrobial property as well as proinflammatory activity [56]. The binding of LL-37 by Pgp3, therefore, may be a strategy employed by *C. trachomatis* to mitigate the host defense mechanism in the genital tract environment. Recently, Hou et al. showed that Pgp3-LL-37 complex abolished the proinflammatory response in vaginal epithelial cells. Intriguingly, the authors found that while Pgp3 alone was unable to trigger the release of IL-6 and IL-8, the binding of Pgp3 with LL-37 increased the release of IL-6 and IL-8 from neutrophils, which may culminate in the onset of inflammatory injury. A likely scenario that emerged from these observations is that Pgp3 dampens the host inflammatory reaction upon release at the site of infection by binding to LL-37 during chlamydial infection. The contact of Pgp3-LL-37 complex with the arriving neutrophils would probably drive the development of inflammatory process [57]. Our results indicated that epithelial cells responded to Pgp3 treatment, which partially contrast with the findings of the previous study. Differences in cell lines used may partially account for this discrepancy. Future studies involving cells and tissues that are more representative of the biology of the natural host of *C. trachomatis*, such as primary cells and organoids, may help to resolve this disparity in results.

In our previous study involving stimulation of peripheral blood mononuclear cells (PBMC) with the chlamydial protease-like activity factor (CPAF), chlamydial heat shock protein 60 (cHSP60), and the major outer membrane (MOMP) of *C. trachomatis*, there was a strong release of proinflammatory cytokines that includes Tumor necrosis factor alpha (TNF $\alpha$ ), IL1 $\beta$ , and IL6. Noteworthy, PBMC derived from patients infected with plasmid-bearing *C. trachomatis* caused a more robust cytokine response [58]. CPAF and cHSP60 are

both known to be potent immunogens in humans [59, 60]. Further, cHSP60 has been shown to induce IL-6 production in a variety of cell types including human endothelial cells, smooth muscle cells, as well as macrophages [61]. Importantly, numerous studies have shown an association between the development of severe reproductive sequelae and the production of antibodies to CPAF and cHSP60 [61–65]. Conceivably, the extracellular release of these chlamydial antigens, including Pgp3, may favor the creation of a proinflammatory environment, leading to the onset of immune-mediated pathology that is associated with chlamydial infection.

## Conclusion

In short, the present investigation demonstrated that Pgp3 plays a likely role in the induction of host inflammatory response during *C. trachomatis* and presented evidence for its possible involvement in the evasion of host immune responses. However, the molecular mechanisms as well as the implication of the release of these cytokines, were not addressed. Further investigation of the molecular pathways and extrapolating the data to an animal model of infection, should be performed. This will prove valuable for decoding the additional functions of Pgp3 protein in order to gain a better insight into the role of the plasmid protein in the pathogenesis of *C. trachomatis*, particularly in the context of chlamydial infection-mediated host immunopathology.

## Abbreviations

ALKBH3	Alkb homolog 3, alpha-ketoglutarate dependent dioxygenase
BRCA2	Breast cancer 2
cHSP60	Chlamydial heat shock protein 60
CHUK	Conserved helix-loop-helix ubiquitous kinase
COMC	Chlamydial outer membrane complex
CPAF	Chlamydial protease-like activity factor
CXCL1	Chemokine C-X-C motif ligand 1
DEAE	Diethylaminoethyl
DMEM	Dulbecco's Modified Eagle Medium
EB	Elementary body
EFNA1	Ephrin A1
FBS	Fetal bovine serum
GM-CSF	Granulocyte-macrophage colony-stimulating factor
GNG12	Protein subunit gamma 12
HBSS	Hank's Balanced Salt Solution
IL	Interleukin
IMAC	Immobilized metal affinity chromatography
IPTG	Isopropyl $\beta$ -D-1-thiogalactopyranoside
IRAK2	Interleukin-1 receptor-associated kinase 2
KDM6A	Lysine-specific demethylase 6A
LPS	Lipopolysaccharide
MALDI-TOF/TOF	Matrix-assisted laser desorption/ionization-tandem time of flight
MOMP	Major outer membrane
MS/MS	Tandem mass spectrometry
ORF	Open reading frames
PBMC	Peripheral blood mononuclear cells
PML	Promyelocytic leukemia
PVDF	Polyvinylidene difluoride

qRT-PCR	Quantitative Real-time polymerase chain reaction
SAT3	Streptothricin-acetyltransferase
SD	Standard deviation
SDS-PAGE	Sodium dodecyl sulfate–polyacrylamide gel electrophoresis
SPG	Sucrose phosphate glutamate buffer
TNFAIP3	Tumor necrosis factor alpha-induced protein 3
TNF $\alpha$	Tumor necrosis factor alpha

## Supplementary Information

The online version contains supplementary material available at <https://doi.org/10.1186/s12866-023-02802-3>.

### Additional file 1.

## Acknowledgements

The authors wish to extend their gratitude to the Malaysian Ministry of Education and University of Malaya Specialist Center (UMSC) for supporting this study, as well as David Chung Tze Yang (Genomax Technologies) for providing assistance in the NanoString analysis.

## Authors' contributions

HCC performed experiments and drafted the manuscript; YYC, YTC, and TTF analyzed the data and prepared the figures; SS and CYL and RG conceived the study and revised the manuscript; BA, LYC and WFW supervised the study. All authors reviewed and approved the manuscript.

## Funding

This study was supported by the Malaysia Ministry of Higher Education Fundamental Research Grant Scheme Grant No: FRGS/1/2020/SKK0/UM/02/10 (FP050–2020). This study is also partially supported by the University of Malaya Specialist Center (UMSC) Care Grant (PV061–2018).

## Availability of data and materials

The datasets used and/or analysed during the current study are available from the corresponding author on reasonable request.

## Declarations

### Ethics approval and consent to participate

Not applicable.

### Consent for publication

Not applicable.

### Competing interests

The authors declare no competing interests.

Received: 10 January 2023 Accepted: 20 February 2023

Published online: 04 March 2023

## References

- Newman L, Rowley J, Vander Hoorn S, Wijesooriya NS, Unemo M, Low N, et al. Global estimates of the prevalence and incidence of four curable sexually transmitted infections in 2012 based on systematic review and global reporting. *PLoS One*. 2015;10:e0143304.
- Ahmadi A, Khodabandehloo M, Ramazan-zadeh R, Farhadifar F, Roshani D, Ghaderi E, et al. The relationship between Chlamydia trachomatis genital infection and spontaneous abortion. *J Reprod Infertil*. 2016;17:110.
- Baud D, Goy G, Jatou K, Osterheld MC, Blumer S, Borel N, et al. Role of Chlamydia trachomatis in miscarriage. *Emerg Infect Dis*. 2011;17:1630.
- Blas MM, Canchihuaman FA, Alva IE, Hawes SE. Pregnancy outcomes in women infected with Chlamydia trachomatis: a population-based cohort study in Washington state. *Sex Transm Infect*. 2007;83:314.
- Rours GI, Duijts L, Moll HA, Arends LR, de Groot R, Jaddoe VW, et al. Chlamydia trachomatis infection during pregnancy associated with preterm delivery: a population-based prospective cohort study. *Eur J Epidemiol*. 2011;26:493.
- Stephens RS. The cellular paradigm of chlamydial pathogenesis. *Trends Microbiol*. 2003;11:44.
- Thomas NS, Lusher M, Storey CC, Clarke IN. Plasmid diversity in Chlamydia. *Microbiology*. 1997;143(Pt 6):1847.
- Gong SQ, Yang ZS, Lei L, Shen L, Zhong GM. Characterization of Chlamydia trachomatis plasmid-encoded open reading frames. *J Bacteriol*. 2013;195:3819.
- Li Z, Chen D, Zhong Y, Wang S, Zhong G. The chlamydial plasmid-encoded protein pgp3 is secreted into the cytosol of Chlamydia-infected cells. *Infect Immun*. 2008;76:3415.
- Chen D, Lei L, Lu C, Galaleldeen A, Hart PJ, Zhong G. Characterization of Pgp3, a Chlamydia trachomatis plasmid-encoded immunodominant antigen. *J Bacteriol*. 2010;192:6017.
- Comanducci M, Manetti R, Bini L, Santucci A, Pallini V, Cevenini R, et al. Humoral immune response to plasmid protein pgp3 in patients with Chlamydia trachomatis infection. *Infect Immun*. 1994;62:5491.
- Ghaem-Maghami S, Ratti G, Ghaem-Maghami M, Comanducci M, Hay PE, Bailey RL, et al. Mucosal and systemic immune responses to plasmid protein pgp3 in patients with genital and ocular Chlamydia trachomatis infection. *Clin Exp Immunol*. 2003;132:436.
- Donati M, Laroucau K, Storni E, Mazzeo C, Magnino S, Di Francesco A, et al. Serological response to pgp3 protein in animal and human chlamydial infections. *Vet Microbiol*. 2009;135:181.
- Li Z, Zhong Y, Lei L, Wu Y, Wang S, Zhong G. Antibodies from women urogenitally infected with C. trachomatis predominantly recognized the plasmid protein pgp3 in a conformation-dependent manner. *BMC Microbiol*. 2008;8:90.
- Scidmore MA. Cultivation and laboratory maintenance of Chlamydia trachomatis. *Curr Protoc Microbiol*. 2005;11:11A.1.
- Jerchel S, Knebel G, Konig P, Bohlmann MK, Rupp J. A human fallopian tube model for investigation of C. trachomatis infections. *J Vis Exp*. 2012;66:e4036.
- Jayapalan JJ, Ng KL, Razack AH, Hashim OH. Identification of potential complementary serum biomarkers to differentiate prostate cancer from benign prostatic hyperplasia using gel- and lectin-based proteomics analyses. *Electrophoresis*. 2012;33:1855.
- Livak KJ, Schmittgen TD. Analysis of relative gene expression data using real-time quantitative PCR and the  $2^{-\Delta\Delta C(T)}$  method. *Methods*. 2001;25:402.
- Duwel M, Welteke V, Oeckinghaus A, Baens M, Kloos B, Ferch U, et al. A20 negatively regulates T cell receptor signaling to NF-kappaB by cleaving Malt1 ubiquitin chains. *J Immunol*. 2009;182:7718.
- Shembade N, Ma A, Harhaj EW. Inhibition of NF-kappaB signaling by A20 through disruption of ubiquitin enzyme complexes. *Science*. 2010;327:1135.
- Porcella SF, Carlson JH, Sturdevant DE, Sturdevant GL, Kanakabandi K, Vir-taneva K, et al. Transcriptional profiling of human epithelial cells infected with plasmid-bearing and plasmid-deficient Chlamydia trachomatis. *Infect Immun*. 2015;83:534.
- Lad SP, Fukuda EY, Li J, de la Maza LM, Li E. Up-regulation of the JAK/STAT1 signal pathway during Chlamydia trachomatis infection. *J Immunol*. 2005;174:7186.
- Qin Y, Li H, Qiao J. TLR2/MyD88/NF-kappaB signalling pathway regulates IL-8 production in porcine alveolar macrophages infected with porcine circovirus 2. *J Gen Virol*. 2016;97:445.
- Rasmussen SJ, Eckmann L, Quayle AJ, Shen L, Zhang YX, Anderson DJ, et al. Secretion of proinflammatory cytokines by epithelial cells in response to Chlamydia infection suggests a central role for epithelial cells in chlamydial pathogenesis. *J Clin Invest*. 1997;99:77.
- Rockey DD. Unraveling the basic biology and clinical significance of the chlamydial plasmid. *J Exp Med*. 2011;208:2159.
- Mitchell CM, Hutton S, Myers GS, Brunham R, Timms P. Chlamydia pneumoniae is genetically diverse in animals and appears to have crossed the host barrier to humans on (at least) two occasions. *PLoS Pathog*. 2010;6:e1000903.
- Jelocnik M, Bachmann NL, Kaltenboeck B, Waugh C, Woolford L, Speight KN, et al. Genetic diversity in the plasticity zone and the presence of the

- chlamydial plasmid differentiates *Chlamydia pecorum* strains from pigs, sheep, cattle, and koalas. *BMC Genomics*. 2015;16:893.
28. Jelocnik M, Bachmann NL, Seth-Smith H, Thomson NR, Timms P, Polkinghorne AM. Molecular characterisation of the *Chlamydia pecorum* plasmid from porcine, ovine, bovine, and koala strains indicates plasmid-strain co-evolution. *PeerJ*. 2016;4:e1661.
  29. Seth-Smith HM, Harris SR, Persson K, Marsh P, Barron A, Bignell A, et al. Co-evolution of genomes and plasmids within *Chlamydia trachomatis* and the emergence in Sweden of a new variant strain. *BMC Genomics*. 2009;10:239.
  30. Jones CA, Hadfield J, Thomson NR, Cleary DW, Marsh P, Clarke IN, et al. The nature and extent of plasmid variation in *Chlamydia trachomatis*. *Microorganisms*. 2020;8:373.
  31. Stothard DR, Williams JA, Van Der Pol B, Jones RB. Identification of a *Chlamydia trachomatis* serovar E urogenital isolate which lacks the cryptic plasmid. *Infect Immun*. 1998;66:6010.
  32. Farencena A, Comanducci M, Donati M, Ratti G, Cevenini R. Characterization of a new isolate of *Chlamydia trachomatis* which lacks the common plasmid and has properties of biovar trachoma. *Infect Immun*. 1997;65:2965.
  33. Peterson EM, Markoff BA, Schachter J, de la Maza LM. The 7.5-kb plasmid present in *Chlamydia trachomatis* is not essential for the growth of this microorganism. *Plasmid*. 1990;23:144.
  34. Buchholz KR, Stephens RS. Activation of the host cell proinflammatory interleukin-8 response by *Chlamydia trachomatis*. *Cell Microbiol*. 2006;8:1768.
  35. Ketriz R, Gaido ML, Haller H, Luft FC, Jennette CJ, Falk RJ. Interleukin-8 delays spontaneous and tumor necrosis factor- $\alpha$ -mediated apoptosis of human neutrophils. *Kidney Int*. 1998;53:84.
  36. Zhang H, Zhou Z, Chen J, Wu G, Yang Z, Zhou Z, et al. Lack of long-lasting hydrosalpinx in a/J mice correlates with rapid but transient chlamydial ascension and neutrophil recruitment in the oviduct following intravaginal inoculation with *Chlamydia muridarum*. *Infect Immun*. 2014;82:2688.
  37. Darville T, Hiltke TJ. Pathogenesis of genital tract disease due to *Chlamydia trachomatis*. *J Infect Dis*. 2010;201(Suppl 2):S114.
  38. Mpiga P, Mansour S, Morisset R, Beaulieu R, Ravaoarino M. Sustained interleukin-6 and interleukin-8 expression following infection with *Chlamydia trachomatis* serovar L2 in a HeLa/THP-1 cell co-culture model. *Scand J Immunol*. 2006;63:199.
  39. Frazer LC, O'Connell CM, Andrews CW Jr, Zurenski MA, Darville T. Enhanced neutrophil longevity and recruitment contribute to the severity of oviduct pathology during *Chlamydia muridarum* infection. *Infect Immun*. 2011;79:4029.
  40. Ramsey KH, Schripsema JH, Smith BJ, Wang Y, Jham BC, O'Hagan KP, et al. Plasmid CDS5 influences infectivity and virulence in a mouse model of *Chlamydia trachomatis* urogenital infection. *Infect Immun*. 2014;82:3341.
  41. Liu Y, Huang Y, Yang Z, Sun Y, Gong S, Hou S, et al. Plasmid-encoded Pgp3 is a major virulence factor for *Chlamydia muridarum* to induce hydrosalpinx in mice. *Infect Immun*. 2014;82:5327.
  42. Kari L, Whitmire WM, Olivares-Zavaleta N, Goheen MM, Taylor LD, Carlson JH, et al. A live-attenuated chlamydial vaccine protects against trachoma in nonhuman primates. *J Exp Med*. 2011;208:2217.
  43. Kawasaki T, Kawai T. Toll-like receptor signaling pathways. *Front Immunol*. 2014;5:461.
  44. Takeda K, Akira S. Toll-like receptors in innate immunity. *Int Immunol*. 2005;17:1.
  45. Joyee AG, Yang X. Role of toll-like receptors in immune responses to chlamydial infections. *Curr Pharm Des*. 2008;14:593.
  46. O'Connell CM, Ionova IA, Quayle AJ, Visintin A, Ingalls RR. Localization of TLR2 and MyD88 to *Chlamydia trachomatis* inclusions. Evidence for signaling by intracellular TLR2 during infection with an obligate intracellular pathogen. *J Biol Chem*. 2006;281:1652.
  47. Darville T, O'Neill JM, Andrews CW Jr, Nagarajan UM, Stahl L, Ojcius DM. Toll-like receptor-2, but not toll-like receptor-4, is essential for development of oviduct pathology in chlamydial genital tract infection. *J Immunol*. 2003;171:6187.
  48. Sturdevant GL, Zhou B, Carlson JH, Whitmire WM, Song L, Caldwell HD. Infectivity of urogenital *Chlamydia trachomatis* plasmid-deficient, CT135-null, and double-deficient strains in female mice. *Pathog Dis*. 2014;71:90.
  49. Sigar IM, Schripsema JH, Wang Y, Clarke IN, Cutcliffe LT, Seth-Smith HM, et al. Plasmid deficiency in urogenital isolates of *Chlamydia trachomatis* reduces infectivity and virulence in a mouse model. *Pathog Dis*. 2014;70:61.
  50. O'Connell CM, AbdelRahman YM, Green E, Darville HK, Saira K, Smith B, et al. Toll-like receptor 2 activation by *Chlamydia trachomatis* is plasmid dependent, and plasmid-responsive chromosomal loci are coordinately regulated in response to glucose limitation by *C. trachomatis* but not by *C. muridarum*. *Infect Immun*. 2011;79:1044.
  51. Russell M, Darville T, Chandra-Kuntal K, Smith B, Andrews CW Jr, O'Connell CM. Infectivity acts as in vivo selection for maintenance of the chlamydial cryptic plasmid. *Infect Immun*. 2011;79:98.
  52. O'Connell CM, Nicks KM. A plasmid-cured *Chlamydia muridarum* strain displays altered plaque morphology and reduced infectivity in cell culture. *Microbiology*. 2006;152:1601.
  53. Carlson JH, Whitmire WM, Crane DD, Wicke L, Virtaneva K, Sturdevant DE, et al. The *Chlamydia trachomatis* plasmid is a transcriptional regulator of chromosomal genes and a virulence factor. *Infect Immun*. 2008;76:2273.
  54. Zhou H, Huang Q, Li Z, Wu Y, Xie X, Ma K, et al. PORF5 plasmid protein of *Chlamydia trachomatis* induces MAPK-mediated pro-inflammatory cytokines via TLR2 activation in THP-1 cells. *Sci China Life Sci*. 2013;56:460.
  55. Hou S, Dong X, Yang Z, Li Z, Liu Q, Zhong G. Chlamydial plasmid-encoded virulence factor Pgp3 neutralizes the antichlamydial activity of human cathelicidin LL-37. *Infect Immun*. 2015;83:4701.
  56. Alalwani SM, Sierigk J, Herr C, Pinkenburg O, Gallo R, Vogelmeier C, et al. The antimicrobial peptide LL-37 modulates the inflammatory and host defense response of human neutrophils. *Eur J Immunol*. 2010;40:1118.
  57. Hou S, Sun X, Dong X, Lin H, Tang L, Xue M, et al. Chlamydial plasmid-encoded virulence factor Pgp3 interacts with human cathelicidin peptide LL-37 to modulate immune response. *Microbes Infect*. 2018;21:50.
  58. Cheong HC, Lee CYQ, Cheok YY, Shankar EM, Sabet NS, Tan GMY, et al. CPAF, HSP60 and MOMP antigens elicit pro-inflammatory cytokines production in the peripheral blood mononuclear cells from genital *Chlamydia trachomatis*-infected patients. *Immunobiology*. 2018;224:34.
  59. Sharma J, Zhong Y, Dong F, Piper JM, Wang G, Zhong G. Profiling of human antibody responses to *Chlamydia trachomatis* urogenital tract infection using microplates arrayed with 156 chlamydial fusion proteins. *Infect Immun*. 2006;74:1490.
  60. Skwor T, Kandel RP, Basravi S, Khan A, Sharma B, Dean D. Characterization of humoral immune responses to chlamydial HSP60, CPAF, and CT795 in inflammatory and severe trachoma. *Invest Ophthalmol Vis Sci*. 2010;51:5128.
  61. Kol A, Bourcier T, Lichtman AH, Libby P. Chlamydial and human heat shock protein 60s activate human vascular endothelium, smooth muscle cells, and macrophages. *J Clin Invest*. 1999;103:571.
  62. Hjelholt A, Christiansen G, Johannesson TG, Ingerslev HJ, Birkelund S. Tubal factor infertility is associated with antibodies against *Chlamydia trachomatis* heat shock protein 60 (HSP60) but not human HSP60. *Hum Reprod*. 2011;26:2069.
  63. Freidank HM, Clad A, Herr AS, Wiedmann-Al-Ahmad M, Jung B. Immune response to *Chlamydia trachomatis* heat-shock protein in infertile female patients and influence of *Chlamydia pneumoniae* antibodies. *Eur J Clin Microbiol Infect Dis*. 1995;14:1063.
  64. van Ess EF, Eck-Hauer A, Land JA, Morre SA, Ouburg S. Combining individual *Chlamydia trachomatis* IgG antibodies MOMP, TARP, CPAF, OMP2, and HSP60 for tubal factor infertility prediction. *Am J Reprod Immunol*. 2019;81:e13091.
  65. Karinen L, Pouta A, Hartikainen AL, Bloigu A, Paldanius M, Leinonen M, et al. Antibodies to *Chlamydia trachomatis* heat shock proteins Hsp60 and Hsp10 and subfertility in general population at age 31. *Am J Reprod Immunol*. 2004;52:291.

## Publisher's Note

Springer Nature remains neutral with regard to jurisdictional claims in published maps and institutional affiliations.